Cell Reports

Article

Mitochondrial gene expression is required for platelet function and blood clotting

Graphical abstract

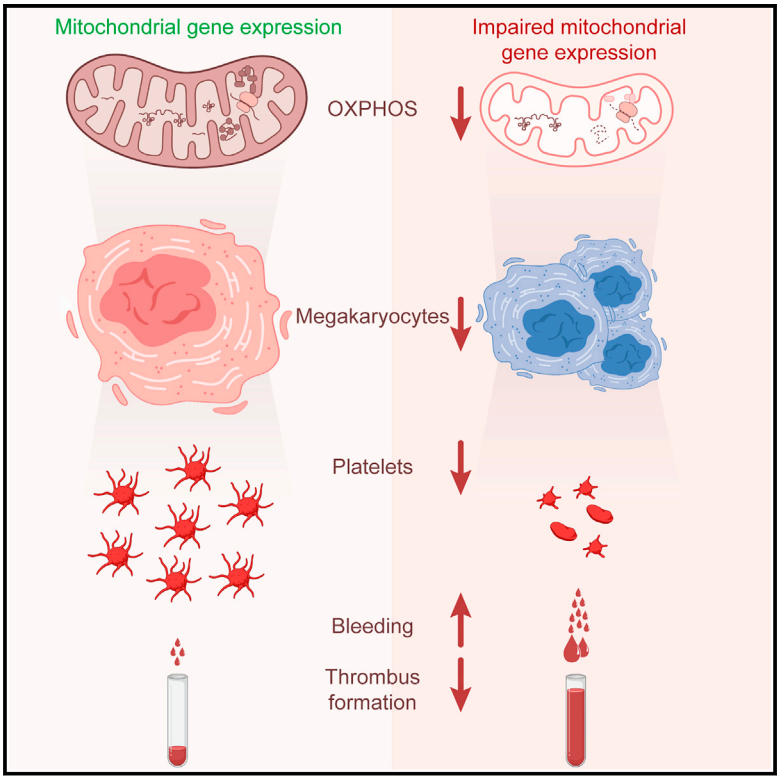

Authors

Tara R. Richman, Judith A. Ermer, Jessica Baker, ..., Matthew D. Linden, Oliver Rackham, Aleksandra Filipovska

Correspondence

aleksandra.filipovska@uwa.edu.au

In brief

Richman et al. specifically delete genes required for mitochondrial gene expression in platelets of mice. They show that mitochondrial RNA-binding proteins (ELAC2, PTCD1, or MTIF3) are essential for platelet activation, megakaryocyte function, and blood coagulation in response to injury. Impaired mitochondrial gene expression leads to thrombocytopenia and excessive bleeding.

Highlights

- Mitochondrial gene expression is required for platelet activation
- ELAC2 is essential for platelet function
- PTCD1 and MTIF3 are essential for both megakaryocyte function and platelet aggregation
- Loss of mitochondrial RNA-binding proteins leads to thrombocytopenia and excessive bleeding

Richman et al., 2023, Cell Reports *42*, 113312
November 28, 2023
https://doi.org/10.1016/j.celrep.2023.113312

CellPress

Cell Reports

CellPress
OPEN ACCESS

Article

Mitochondrial gene expression is required for platelet function and blood clotting

Tara R. Richman,[1,2,3,4,9] Judith A. Ermer,[1,2,3,9] Jessica Baker,[1,2,3,4] Stefan J. Siira,[1,2,3,4] Benjamin T. Kile,[5] Matthew D. Linden,[6] Oliver Rackham,[1,2,4,7,8] and Aleksandra Filipovska[2,4,10,11,*]

[1]Harry Perkins Institute of Medical Research, QEII Medical Centre, Nedlands, WA 6009, Australia
[2]ARC Centre of Excellence in Synthetic Biology, QEII Medical Centre, Nedlands, WA 6009, Australia
[3]Centre for Medical Research, The University of Western Australia, QEII Medical Centre, Nedlands, WA 6009, Australia
[4]Telethon Kids Institute, Northern Entrance, Perth Children's Hospital, 15 Hospital Avenue, Nedlands, WA, Australia
[5]Faculty of Health and Medical Sciences, University of Adelaide, Adelaide, SA 5005, Australia
[6]Pathology and Laboratory Science, The University of Western Australia, Perth, WA, Australia
[7]Curtin Medical School, Curtin University, Bentley, WA 6102, Australia
[8]Curtin Health Innovation Research Institute, Curtin University, Bentley, WA 6102, Australia
[9]These authors contributed equally
[10]Senior author
[11]Lead contact
*Correspondence: aleksandra.filipovska@uwa.edu.au
https://doi.org/10.1016/j.celrep.2023.113312

SUMMARY

Platelets are anucleate blood cells that contain mitochondria and regulate blood clotting in response to injury. Mitochondria contain their own gene expression machinery that relies on nuclear-encoded factors for the biogenesis of the oxidative phosphorylation system to produce energy required for thrombosis. The autonomy of the mitochondrial gene expression machinery from the nucleus is unclear, and platelets provide a valuable model to understand its importance in anucleate cells. Here, we conditionally delete *Elac2*, *Ptcd1*, or *Mtif3* in platelets, which are essential for mitochondrial gene expression at the level of RNA processing, stability, or translation, respectively. Loss of ELAC2, PTCD1, or MTIF3 leads to increased megakaryocyte ploidy, elevated circulating levels of reticulated platelets, thrombocytopenia, and consequent extended bleeding time. Impaired mitochondrial gene expression reduces agonist-induced platelet activation. Transcriptomic and proteomic analyses show that mitochondrial gene expression is required for fibrinolysis, hemostasis, and blood coagulation in response to injury.

INTRODUCTION

Platelets are small, anucleate cells that play essential roles in blood clotting, wound healing, and the response to infection. They are generated by megakaryocytes, large, polyploid hematopoietic precursor cells that develop primarily in the bone marrow, but they are also present in the spleen[1] and in the lungs.[2] The megakaryocyte lineage has its origins in the hematopoietic stem cell, which is driven toward megakaryocyte production by the cytokine thrombopoietin.[3] Polyploidization is accompanied by a dramatic expansion of cytoplasmic volume that allows each megakaryocyte to produce hundreds, perhaps thousands, of platelets via cytoplasmic protrusions or membrane budding.[4]

Given they lack a nucleus, the function of mammalian platelets is regulated at the posttranscriptional level via protein phosphorylation and through messenger RNAs (mRNAs), ribosomes, and microRNAs (miRNAs) within their cytoskeletal protein-rich cytoplasm that is retained during budding off from the megakaryocyte.[1] Platelets turn over adenosine triphosphate (ATP) at a greater rate than resting mammalian myocytes.[5] This high energy demand in platelets is met by glycolysis and mitochondrial oxidative phosphorylation (OXPHOS).[6] The biogenesis of the OXPHOS system in mitochondria is dependent on the coordinated expression of both nuclear and mitochondrial genes.[7] However, the role and requirement for mitochondrial gene expression in platelets are not known.

The molecular systems that regulate mitochondrial gene expression are unique and require diverse nuclear-encoded RNA-binding proteins (RBPs) to produce and regulate the mitochondrial transcriptome.[7] Mitochondrial genomes are transcribed as long, near genome-sized polycistronic transcripts that are then processed predominantly by the tRNA endonucleases RNase P and RNase Z, which cleave and release the mitochondrial RNAs (mt-RNAs) into smaller functional units.[8–10] Mitochondrial mRNAs, tRNAs, and rRNAs are then modified and matured by a range of different enzymes to form a complete mitochondrial translation system for the synthesis of the 13 polypeptides required for the biogenesis of the OXPHOS system.[7] The majority of OXPHOS proteins along with all other mitochondrial proteins are nuclear-encoded and post-translationally imported into mitochondria. Consequently, mitochondrial gene expression

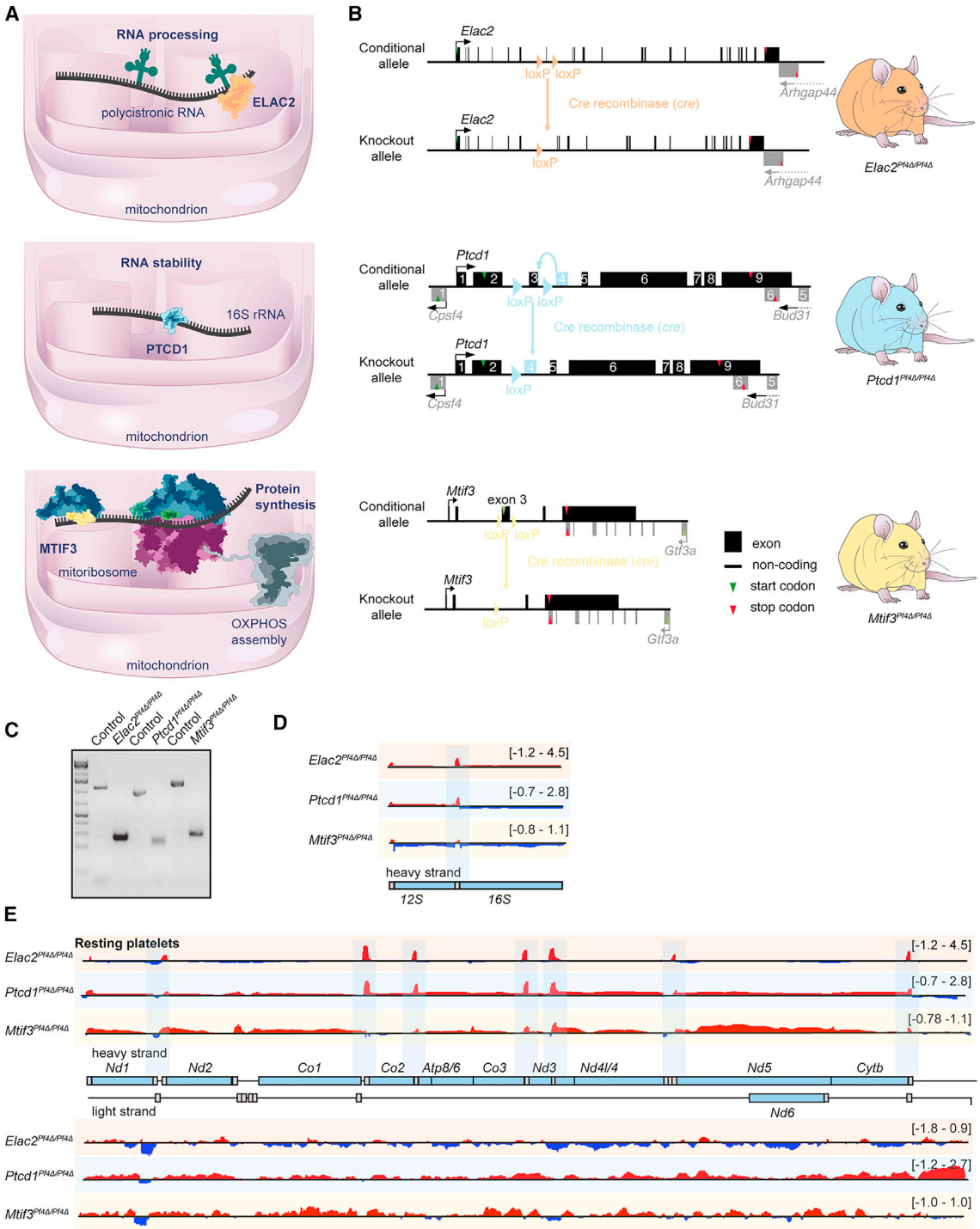

Figure 1. Loss of mitochondrial RNA-binding proteins causes transcript specific defects in platelets

(A) ELAC2, PTCD1, and MTIF3 are nuclear-encoded mitochondrial RNA-binding proteins that regulate tRNA processing, rRNA stability, and protein synthesis, respectively.

(B) Schematics showing the homologous recombination at each of the gene loci used to generate conditional knockout mice. *LoxP* sites were introduced to allow the specific deletion of the highlighted exons in platelets by Pf4 promoter-driven expression of a Cre recombinase to generate *Elac2*$^{Pf4\Delta/Pf4\Delta}$, *Ptcd1* $^{Pf4\Delta/Pf4\Delta}$, and *Mtif3* $^{Pf4\Delta/Pf4\Delta}$ mouse lines.

(C) PCR confirming specific deletion of targeted exons within the *Elac2*, *Ptcd1*, and *Mtif3* genes in megakaryocytes. Data are representative of n ≥ 3 mice per genotype.

(D) Changes in mitochondrial RNA precursor abundance determined by RNA-seq coverage from three control (L/L) and three of knockout (L/L, Cre) mice on heavy (upper track) and light (lower track) strands. Increases are shown in red, and decreases are shown in blue (expressed as $\log_2$ fold change of each genotype relative

(legend continued on next page)

is tightly coordinated with nuclear gene expression to enable the assembly of the mitochondrial ribosomes and OXPHOS complexes.[11] Loss of nuclear-encoded proteins involved in the gene expression machinery of mitochondria in model organisms or patient cells has contributed significant knowledge about the regulation of the mitochondrial genome,[7,12] but little is known about their role in platelet formation and function.

Here, we generated three megakaryocyte/platelet-specific conditional knockout mouse lines that impair three different stages of mitochondrial gene expression to investigate the importance of mitochondrial RNA metabolism for platelet function. We show that mitochondrial gene expression is required for platelet function. Impaired mitochondrial gene expression caused thrombocytopenia, increased bleeding time, and higher platelet turnover as a consequence of megakaryopoiesis and increased megakaryocyte ploidy. Furthermore, we show that the severity of platelet and megakaryocyte dysfunction reflects specific defects in mitochondrial RNA metabolism that affect different thrombosis pathways during platelet activation.

RESULTS

Loss of mitochondrial RNA-binding proteins in platelets causes defects in mitochondrial gene expression

To investigate mitochondrial gene expression in platelets, we knocked out the nuclear-encoded RBPs ELAC2, PTCD1, and MTIF3 (Figure 1A). These are essential regulators of the life cycles of mitochondrial RNAs (mt-RNAs), from RNA processing and stability to translation.[10,11,13] *Elac2* encodes RNase Z, which is essential for tRNA processing and release of individual mitochondrial mRNAs, tRNAs, and rRNAs from the polycistronic transcripts as well as nuclear tRNAs.[10] The *Ptcd1* gene encodes a scaffold protein required for mitochondrial 16S rRNA stability and maturation.[13] Mitochondrial protein synthesis was targeted by deletion of the mitochondrial translation initiation factor 3 gene, *Mtif3*.[11] Loss of each of the three genes causes embryonic lethality[10,11,13]; therefore we generated three conditional platelet-specific deletions of each gene (*Elac2*$^{Pf4\Delta/Pf4\Delta}$, *Ptcd1* $^{Pf4\Delta/Pf4\Delta}$, and *Mtif3* $^{Pf4\Delta/Pf4\Delta}$) by crossing mice containing *loxP* sites that flanked essential exons with transgenic mice expressing the Cre recombinase under the control of the platelet factor 4 (*Pf4*) promoter (Figure 1B), which effectively recombined each of the genes in megakaryocytes (Figure 1C).

RNA sequencing (RNA-seq) of resting platelets isolated from 4-week-old knockout mice compared to controls revealed defects in the mitochondrial transcriptomes specific to each gene deletion (Figures 1D and 1E). In the resting platelets of the *Elac2* knockout mice, there was marked accumulation of tRNA precursors that indicated impaired tRNA processing compared to control platelets (Figures 1D and 1E), consistent with changes previously identified in heart- and skeletal muscle-specific deletion of *Elac2*.[10] Decreased stability of the 16S rRNA along with tRNA precursor accumulation was found in the platelets of the *Ptcd1* knockout mice (Figure 1D), similar to defects identified in heart and liver mitochondria isolated from mice that have heterozygous or homozygous loss of PTCD1.[13,14] Increased mitochondrial mRNA and decreased rRNA expression were found in resting platelets from the *Mtif3* knockout mice (Figures 1D–1E and S1). The molecular defects caused by loss of each protein in the platelets were consistent with other tissues,[10,11,13] indicating conservation of their roles in mitochondrial gene expression.

Loss of ELAC2, PTCD1, or MTIF3 causes thrombocytopenia and elevated levels of reticulated platelets

Platelet numbers were significantly reduced in 4-week-old *Elac2, Ptcd1*, and *Mtif3* knockouts compared to gender- and age-matched littermate control mice (Figure 2A), while red and white blood cell numbers were comparable between control and knockout mice (Figures 2B and 2C). Despite the reduced platelet counts, blood films revealed similar platelet morphologies between the knockout and control mice (Figure 2D). These findings indicate that megakaryocyte- and platelet-specific loss of ELAC2, PTCD1, or MTIF3 result in thrombocytopenia in all three knockout models. Tail bleeding tests showed that the *Elac2*, *Ptcd1*, and *Mtif3* knockout mice bled for a significantly longer time compared to their age-matched controls (Figure 2E) and had a significantly higher bleeding index (Figure 2F), consistent with the development of thrombocytopenia.

Platelets newly released to the circulation can be identified as they are larger, more reactive, and contain RNA. These reticulated platelets (RPs) or immature platelets circulate for 24–36 h in this reticulated state before progressive degradation of RNA, and a decrease in volume sees them take on the morphology of a mature platelet, which continues to circulate for a further 7–10 days.[15] Therefore, the number of RPs is indicative of active thrombopoiesis. An elevated immature platelet fraction (IPF) is common with reactive thrombopoiesis, following increased platelet destruction in conditions like immune thrombocytopenia (ITP).[15] We used thiazole orange to measure RPs and found that loss of ELAC2, PTCD1, or MTIF3 caused an increase in IPFs compared to controls (Figure 2G), consistent with reduced number of mature platelets and increased bleeding, suggesting that these proteins are required for platelet hemostasis and turnover (Figure 2G).

Megakaryopoiesis is impaired in *Mtif3* and *Ptcd1* knockout mice

Megakaryocyte colony assays were performed on bone marrow cells isolated from each of the three knockout and control mice to determine if impaired megakaryopoiesis contributed to thrombocytopenia. *Elac2* knockout mice had similar numbers of small and large megakaryocyte (Mk) colonies compared to controls (Figure 3A), indicating that loss of ELAC2 did not inhibit Mk production. However, in the *Ptcd1* knockout mice, there were

to control mean counts per million, plus a pseudocount of 1; log2[(RPM^{KO}+1)/(RPM^{WT}+1)]). The mitochondrial genome is displayed in the central track; mRNAs and rRNAs are in blue, and tRNAs are in gray. The tRNA junctions that separate the mRNAs and rRNAs are marked in transparent blue boxes, and the specific enrichment of these regions indicates accumulation of processing intermediates and thereby impaired RNA processing.

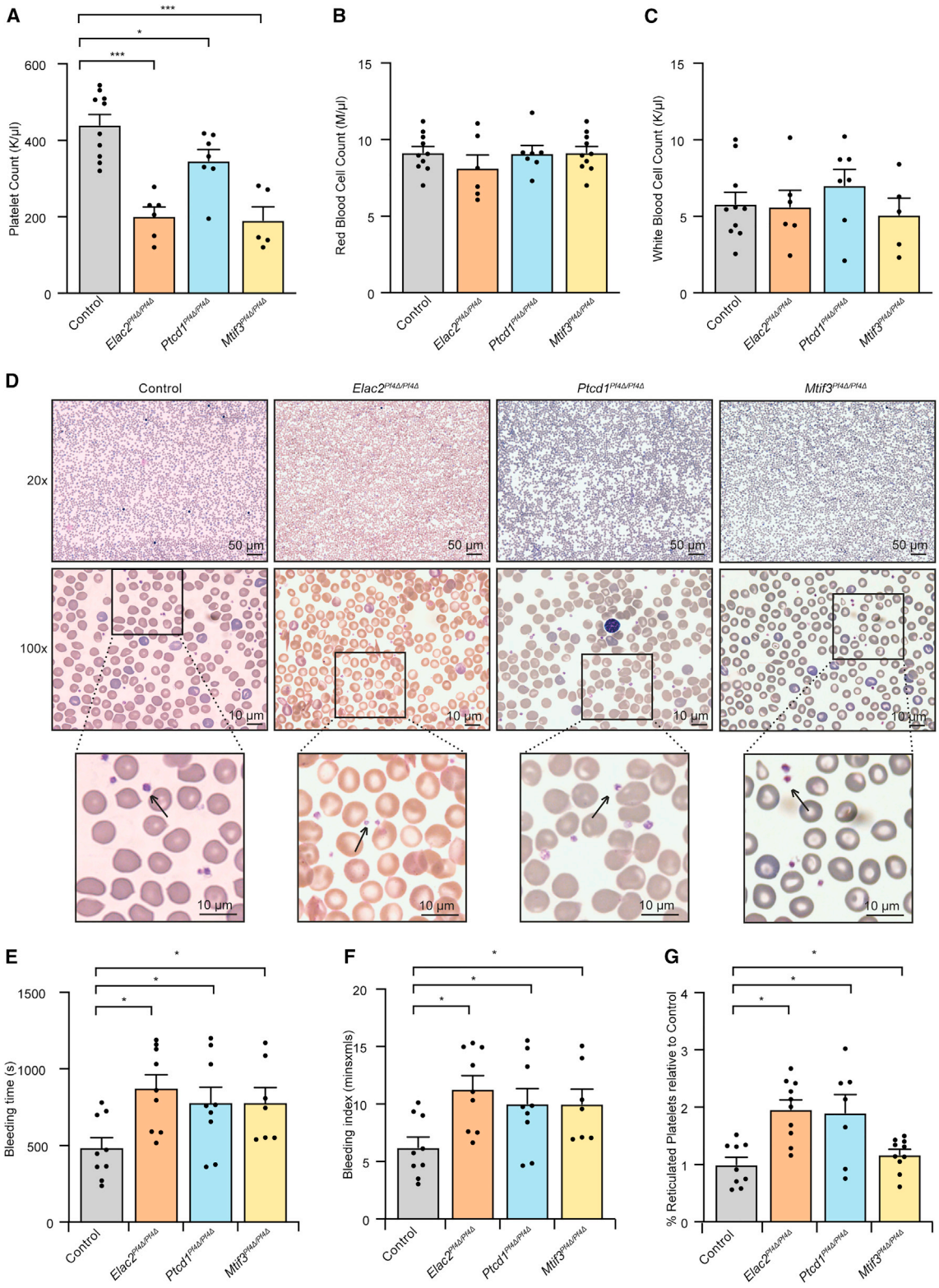

Figure 2. Knockout of *Elac2*, *Ptcd1*, and *Mtif3* causes reduced platelet counts with increased bleeding and percentage of reticulated platelets

(A) Whole blood counts and blood cell morphology were analyzed in mice at 4 weeks of age. Platelet counts were significantly reduced in *Elac2*, *Ptcd1*, and *Mtif3* knockout mice at 4 weeks of age compared to control mice.

(legend continued on next page)

significantly fewer large megakaryocyte colonies (Figure 3B), and in the *Mtif3* knockout mice, there were significantly lower numbers of both small and large megakaryocyte progenitor colonies (Figure 3C) compared to their respective control mice (Figure 3D). Therefore, loss of PTCD1 or MTIF3 causes reduced megakaryopoiesis that contributes to thrombocytopenia.

We used acetylthiocholine iodide to investigate megakaryocyte morphology in bone marrow, spleen, and lungs isolated from control and each of the knockout mouse lines. Bone marrow megakaryocytes from *Elac2*, *Ptcd1*, and *Mtif3* mice appeared larger, more lobated, and with more abundant cytoplasm than those seen in the control (Figure 3E) and significantly reduced proplatelet forming megakaryocytes (Figure 3F), while the morphology of the spleen and lung megakaryocytes was comparable between the control and each of the three knockout lines (Figures 3G and 3H). Next, we examined the megakaryocyte ploidy profiles to determine if megakaryocyte maturation was impaired in the knockout mouse lines in bone marrow cells isolated from control and each of the knockout mouse lines. 16N-containing megakaryocytes from *Elac2* and *Mtif3* knockout mice were significantly reduced, while >32N-containing megakaryocytes were significantly increased in all knockout lines (Figure 3I). These results revealed a deficiency in megakaryocyte differentiation potential in the *Ptcd1* and *Mtif3* mice, consistent with reduced megakaryopoiesis, and significantly increased megakaryocyte ploidy in all knockout mouse lines, likely as a compensatory mechanism for the significant reduction in platelet numbers and consistent with the development of thrombocytopenia in these mice.

Loss of ELAC2, PTCD1, or MTIF3 impairs platelet activation

To elucidate the pathways affected by loss of ELAC2, PTCD1, and MTIF3, we measured platelet activation in response to low and high concentrations of four different agonists administered to isolated platelets from control, *Elac2, Ptcd1,* and *Mtif3* knockout mice. Platelet function was measured by membrane P-selectin expression in response to canonical platelet agonists: (1) Ala-Tyr-Pro-Gly-Lys-Phe-NH_2 (AYPGKF), the most potent platelet PAR4 agonist that stimulates thromboxane production in platelets[16]; (2) adenosine diphosphate (ADP), a comparatively mild platelet agonist that is a dense granule exocytosis mediator causing activation through P2Y receptors[17]; (3) arachidonic acid (ARA), which is metabolized through a cyclo-oxygenase-1 (COX1)-dependent pathway to produce thromboxane A_2 causing platelet activation, recruitment, and thrombus consolidation via the thromboxane receptor[18]; and (4) collagen that activates the platelet glycoprotein VI (GPVI) receptor-mediated signaling pathway in platelets via the spleen tyrosine kinase (Syk) and phospholipase C-γ2 (PLC-γ2), which leads to thromboxane A_2 synthesis and granule secretion.[19]

Platelet function was severely compromised at both low and high concentrations of AYPGKF in platelets isolated from *Elac2* knockout mice (Figure 4A). Platelets isolated from the *Ptcd1* knockout mice had decreased sensitivity to low and high concentrations of ADP (Figure 4B). *Mtif3* knockout mice showed impaired platelet activation in response to both low and high concentrations of AYPGKF, similar to the *Elac2* knockout mice, with an additional defective response to ARA at high concentration (Figure 4C). These results suggest a loss of PAR4 signaling in the absence of ELAC2, confirmed further by significant reduction in ERK1/2 signaling, as the downstream target in the PAR4 pathway (Figure S2), or MTIF3, a defect in the thromboxane pathway in the *Mtif3* knockout mice, and a P2Y receptor signaling defect in the *Ptcd1* knockout mice.

Mitochondrial levels were significantly reduced in both resting and activated platelets isolated from the knockout lines compared to control platelets (Figure 4D), indicating that loss of each mitochondrial RBP compromised mitochondrial function and contributed to impaired platelet numbers. Furthermore, there was increased apoptotic cell death in the resting platelets from each of the knockout lines compared to controls (Figure 4E), suggesting that high mitochondrial content is necessary for platelet viability. However, there was comparable cell death between control and each of the knockout line platelets in the presence of the activation agonist, indicating that although viability is affected by the reduction of mitochondrial content, the sensitivity of these platelets to cell death during responses to canonical agonists is not. Finally, the levels of mitochondrial proteins including the mitochondrially encoded cytochrome *c* oxidase subunit II (COXII) polypeptide were reduced in the platelets from all three KO lines, further confirming that defects in mitochondrial gene expression contributed to reduced platelet function (Figure S3).

Impaired mitochondrial gene expression causes transcriptome- and proteome-wide changes in megakaryocytes and activated platelets

We used the AYPGKF agonist to investigate the effects of platelet activation on mitochondrial gene expression in the knockout mice compared to controls. In the knockout mice, we found similar mitochondrial transcriptome defects in activated platelets as those in non-activated platelets, where loss of ELAC2 caused impaired processing of the 3′ ends of tRNAs, and loss of PTCD1 resulted in decreased 16S rRNA levels (Figures 5A, S4, and S5; Table S1). However, in the activated platelets from the *Mtif3* knockout mice, in the absence of MTIF3 and impaired translation initiation, mitochondrial mRNA and rRNA levels were reduced (Figure 5A), indicating that mitochondrial translation is required

(B and C) Red (B) and white (C) cell counts were comparable between control and *Elac2*, *Ptcd1*, or *Mtif3* knockout mice. All values are means ± SEM of $n \geq 6$, *$p < 0.05$, **$p < 0.01$, ***$p < 0.001$, Student's t test.

(D) Quick Dip Kit-stained blood films from *Elac2, Ptcd1*, and *Mtif3* knockout mice show comparable platelet morphology to control mice. Images are representative of samples collected from $n \geq 6$ mice.

(E) Bleeding time was measured in control and knockout mice over 20 min.

(F) The bleeding index of knockout compared to control mice was determined as volume of blood collected per 20 min.

(G) Percent of reticulated platelets in *Elac2*, *Ptcd1*, and *Mtif3* mice compared to controls at 4 weeks of age. All values are means ± SEM of $n \geq 6$, *$p < 0.05$, **$p < 0.01$, ***$p < 0.001$, Student's t test.

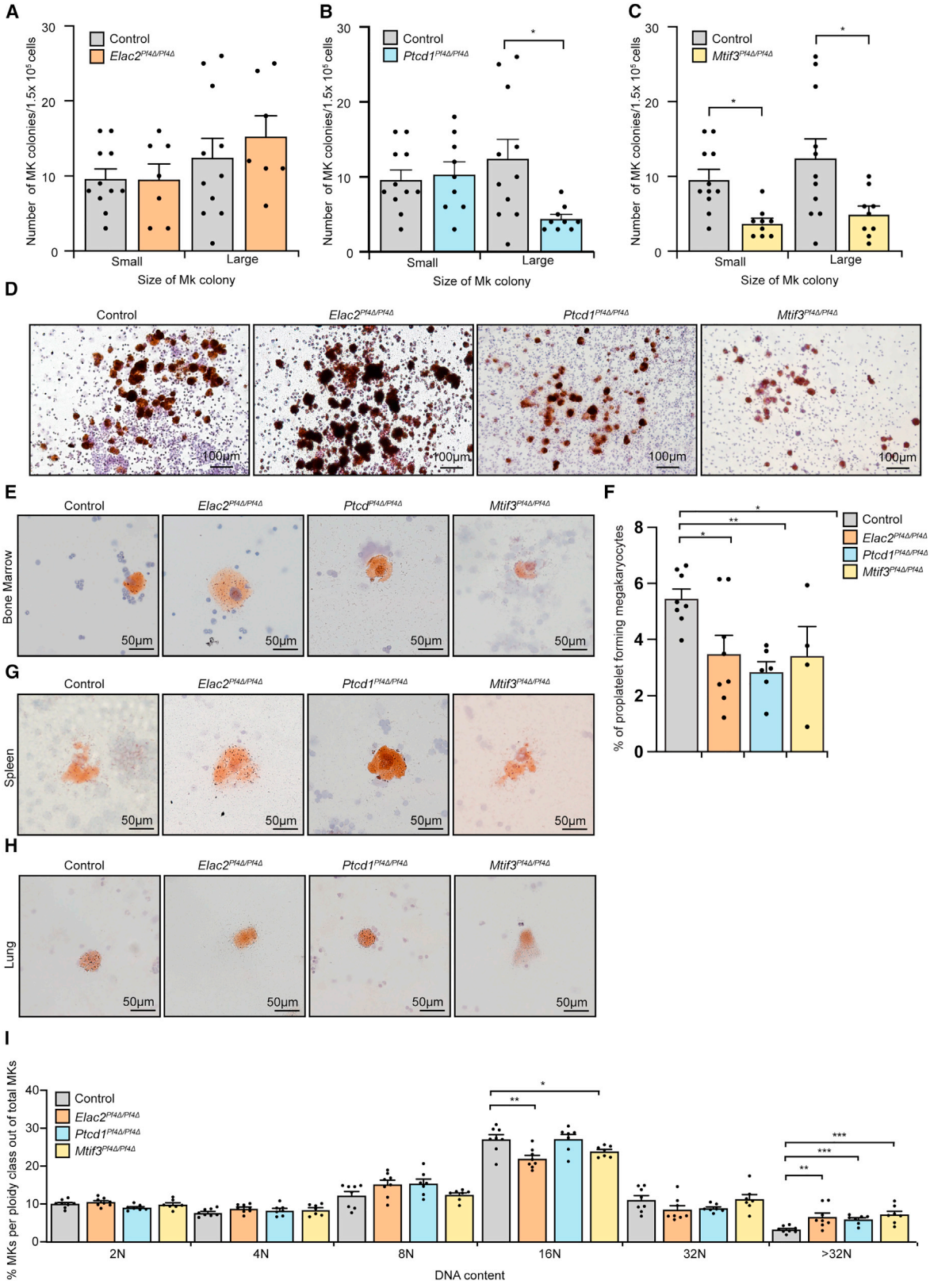

(legend on next page)

during platelet activation. RNA-seq of megakaryocytes from each of the mouse lines revealed similar mitochondrial transcriptome changes in each respective line (Figure 5B), mirroring those in the activated platelets (Figure 5A). These findings confirm that the platelet and megakaryocyte defects in the knockout mice are a consequence of impaired mitochondrial gene expression.

Next, we investigated the consequences of ELAC2, PTCD1, or MTIF3 loss on nuclear gene expression in resting and activated platelets and megakaryocytes (Figures 6, S6A, and S6B). Differential gene expression analyses of megakaryocyte transcriptomes in *Elac2* knockout mice showed the most significant gene changes related to chemotaxis (Figures 6A and S7). Minimal transcriptome changes were observed in the megakaryocytes of the *Ptcd1* knockout mice (Figure 6B), and transcriptional changes seen in the activated platelets included mostly translation and mitochondrial biogenesis genes such as *Tfam*, important in mitochondrial DNA replication and repair (Figure S6B). The *Mtif3* knockout mice had the largest number of transcriptional changes in megakaryocytes (Figure 6C), and these affected genes involved in thrombin receptor signaling, platelet formation, megakaryocyte development, hemostasis, complement activation, hematopoiesis, and blood coagulation (Figure S7).

We used label-free quantitative proteomics to investigate changes at the protein level in platelets lacking each of the mitochondrial RBPs in the presence or absence of the AYPGKF agonist to relate our results to the observed activation defects. In resting platelets, there were no significant changes between control and each of the knockout mouse lines, suggesting that mitochondrial gene expression does not affect total protein levels. Since resting platelets have low translational activity and it is upon activation that rapid translation is triggered,[20] we profiled the proteomes of activated platelets and their secreted proteins, where we identified markedly different profiles between each of the knockout lines (Table S2). Loss of ELAC2 resulted in changes in proteins involved in fibrinolysis, erythrocyte development, and hemostasis (Figure 6D). Specific changes included increased levels of plasma kallikrein (KLKB1) and coagulation factor XII (F12), both of which have roles in coagulation and fibrinolysis and potential activation of an immune response via the kallikrein-kinin system.[21] The platelet alpha granule proteins released following thrombin stimulation, HRG, SERPINA1E, and SERPINA10, were increased in the *Elac2* knockout mice (Figure 6D). Decreased levels of the mitochondrial proteins PRDX2, HSP90B1, and PGK1 and hemoglobin subunits (HBB-B1 and HBA-A1) were consistent with defects in mitochondrial function and thrombocytopenia in the *Elac2* knockout mice (Figure 6D), as PRDX2 is required for hydrogen peroxide detoxification and regulation of platelet-derived growth factor signaling,[22] and HSP90B1 is essential in the formation of the platelet glycoprotein Ib-IX (GPIB-IX). Furthermore, reduction in PGK1, which phosphorylates pyruvate dehydrogenase kinase, contributed to impaired platelet function, as did reduced CA2 (Figure 6D), which lowers the cytosolic pH in platelets by catalyzing the formation of H^+ and HCO_3^-.[23]

There were no significant changes in the platelet proteomes of the *Ptcd1* mice, likely as they have a similar response to the agonist as the control mice. However, in the *Mtif3* knockout mice, there was a significant reduction of the mitochondrial proteins HSP90B1 and MDH2 and reduced levels of proteins required for platelet activation via integrin signaling such as TLN1 (talin1) and granule secretion including PDIA6 (Figure 6E). The abundance of cytoskeletal and actin-binding proteins required for the cytoskeletal architecture of platelets, including WDR1, CAP1, and TPM4, was reduced with the most significant proteome changes affecting glycolysis (Figure 6E). The proteome changes are consistent with thrombocytopenia and the blood clotting defects identified in mice lacking ELAC2 or MTIF3, indicating that these proteins are required for mitochondrial gene expression during platelet activation.

We integrated transcriptome and proteome changes observed in activated platelets and megakaryocytes to identify the pathways by which each of the mitochondrial RBP led to thrombocytopenia (Figure 6F). Loss of ELAC2 caused increased protein expression in HRG (platelet dense granule contents) and kinin-kallikrein system proteins, F12, KLKB1, and proteins involved in the complement cascade (H2-BF, C4). This was consistent with the observed platelet-specific defect in mice lacking ELAC2. In the megakaryocytes, loss of PTCD1 caused transcriptional changes that led to decreased expression of the complement cascade (*C3ar1*) and *Cyp11a1* and an increase in mRNAs involved in the Gq/G11 and prostaglandin pathway (*Ptgdr*). Activated platelets from *Ptcd1* knockout mice had reduced expression of prostaglandin pathway mRNAs, *Ephx2*, *Ptgis*, and *Ptger4*, which are also involved in the Gq/G11 pathway (Figure 6F).

Figure 3. MTIF3 and PTCD1 loss causes megakaryopoiesis

(A–C) 2.5 x 10^5 bone marrow cells were cultured at 37°C in the presence of cytokines at 5% CO_2 for 7 days. CFU-Mks were stained with acetylthiocholine iodide and the number of small (3–20 cells per colony) and large (>20 cell per colony) colonies were counted in *Elac2* (A), *Ptcd1* (B), and *Mtif3* (C) knockout mice compared to controls. All values are means ± SEM of $n \geq 6$, *$p < 0.05$, **$p < 0.01$, ***$p < 0.001$, Student's t test.

(D) Representative images of megakaryocyte colonies from at least six mice stained with acetylthiocholine iodide (brown) for each genotype.

(E) Morphologies of bone marrow megakaryocytes. Representative images of acetylthiocholine iodide staining of slides from at least six mice, prepared by centrifuging bone marrow single-cell suspensions onto slides using a Cytospin centrifuge.

(F) Percent of proplatelet megakaryocytes were quantitated; all values are means ± SEM of $n \geq 4$, *$p < 0.05$, **$p < 0.01$, Student's t test.

(G) Morphologies of spleen megakaryocytes. Representative images of acetylthiocholine iodide staining of slides prepared by centrifuging single-cell suspensions prepared from spleen onto slides using a Cytospin centrifuge. Images are representative of $n \geq 6$ mice.

(H) Morphologies of lung megakaryocytes. Representative images of acetylthiocholine iodide staining of slides prepared by centrifuging single-cell suspensions prepared from spleen onto slides using a Cytospin centrifuge. Images are representative of $n \geq 6$ mice.

(I) Megakaryocyte ploidy. Bone marrow cells from all three knockout mice were collected and stained with CD41-FITC, IgG-FITC, and propidium iodide (PI). Cells were gated using IgG-FITC and confirmed with a positive CD41-FITC sample. High $CD41^+$ events were counted and 2N population was based on lymphocyte gate (FSC/SSC plot). Quantification of ploidy status per group was determined as a percentage of cells in the $CD41^+$ megakaryocyte gate. All values are means ± SEM of $n \geq 7$, *$p < 0.05$, **$p < 0.01$, ***$p < 0.001$, Student's t test.

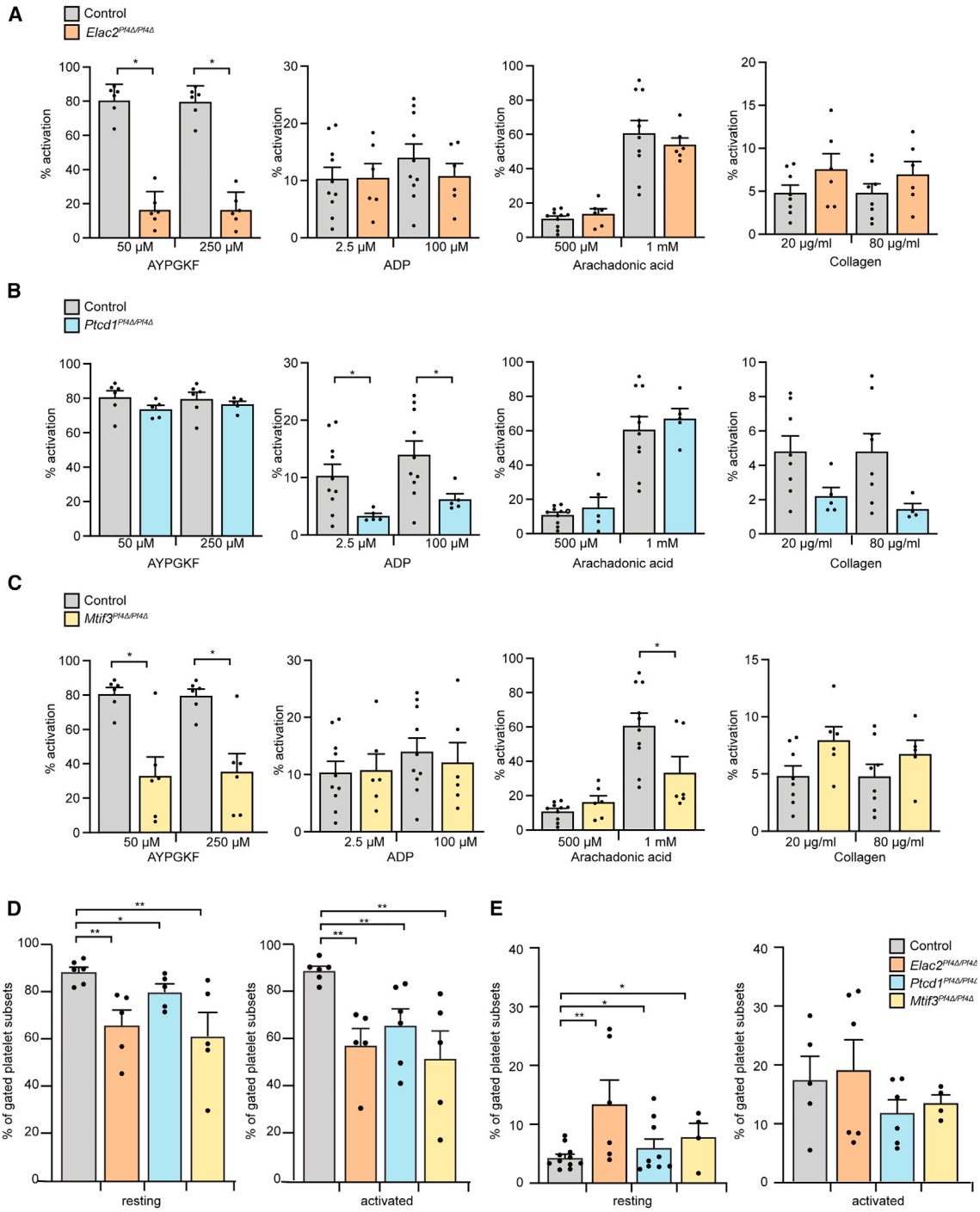

Figure 4. *Elac2, Ptcd1*, and *Mtif3* loss leads to altered agonist sensitivity

(A) Isolated platelets were activated with a panel of agonists, AYPGKF, ARA, and collagen, and analyzed for P-selectin externalization by flow cytometry. Platelets isolated from *Elac2* knockout mice showed decreased sensitivity to AYPGKF at low and high concentrations.

(B) Platelets isolated from *Ptcd1* knockout mice and exposed to low and high concentrations of ADP had decreased sensitivity.

(C) Platelets isolated from *Mtif3* knockout mice caused a decrease in sensitivity to AYPGKF at low and high concentrations and ARA at high concentrations. Values in all panels are means ± SEM of $n \geq 6$, *$p < 0.05$, **$p < 0.01$, ***$p < 0.001$, Student's t test.

(D) Percent of isolated platelets (resting or activated with AYPGKF) stained with Mitotracker Green analyzed by flow cytometry. All values are means ± SEM of $n \geq 5$, *$p < 0.05$, **$p < 0.01$, ***$p < 0.001$, Student's t test.

(E) Percent of isolated platelets (resting or activated) stained with Annexin V in controls and *Elac2*, *Ptcd1*, and *Mtif3* knockout mice, analyzed by flow cytometry. All values are means ± SEM of $n \geq 4$, *$p < 0.05$, **$p < 0.01$, ***$p < 0.001$, Student's t test.

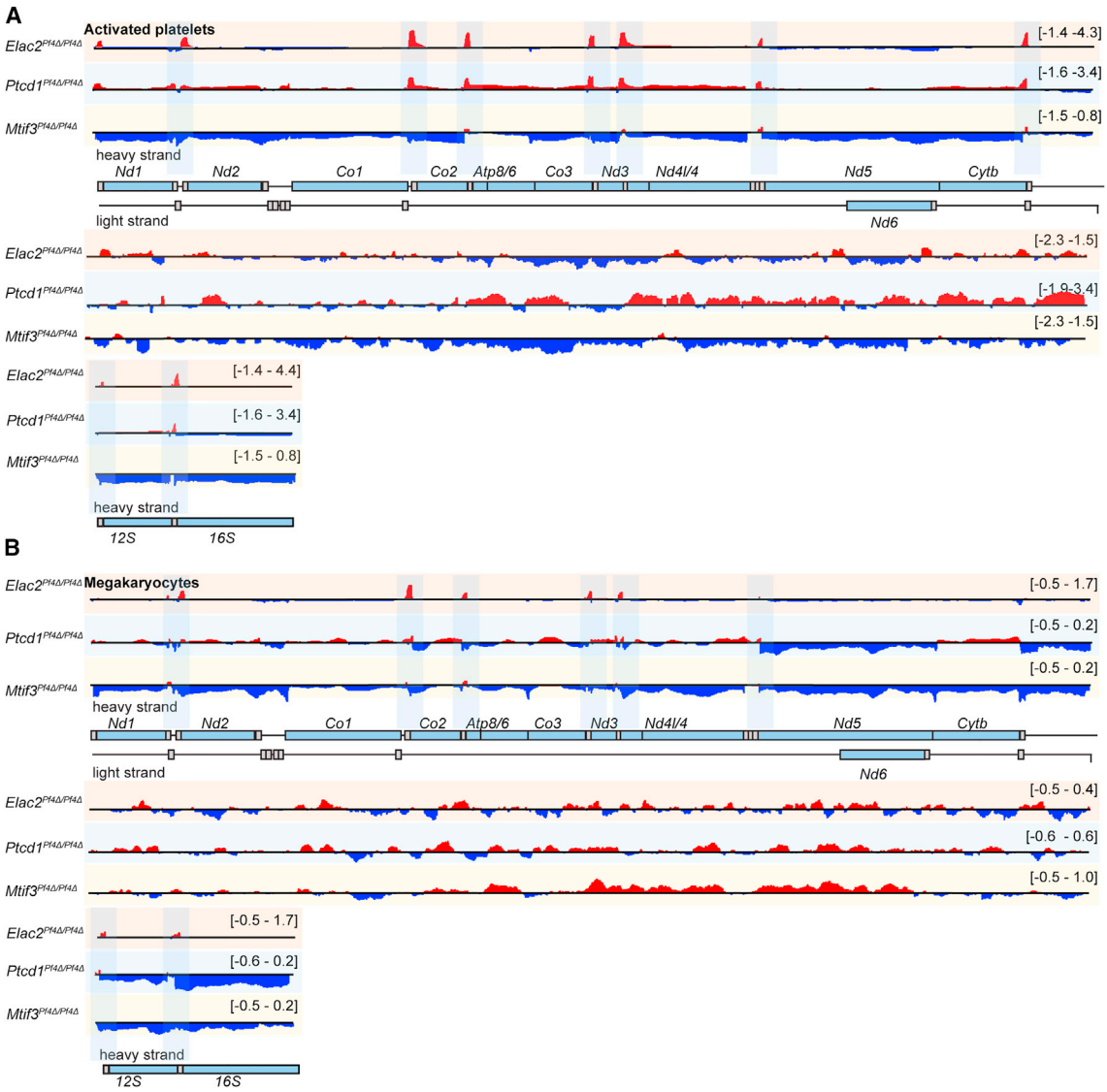

Figure 5. Mitochondrial gene expression changes during platelet activation

(A and B) Changes in mitochondrial coverage profiles (expressed as $\log_2$ fold change of the per condition mean counts per million, plus a pseudo count of 1; $\log_2[(RPM^{KO}+1)/(RPM^{WT}+1)]$) in (A) platelets activated with 250 μM AYPGKF agonist and (B) megakaryocytes from three control and three knockout mice from each line were determined by RNA-seq. The expression profiles of the heavy (upper tracks) and light (lower tracks) strands are shown as increases in red and decreases in blue. The mitochondrial genome is displayed in the central track; mRNAs and rRNAs are in blue, and tRNAs are in gray.

MTIF3 loss caused reduction of the coagulation cascade (*F2r, Vwf*), the kinin-kallikrein system (*Pros1*), the complement cascade (*C1qa, C1qb, C1qg*), the Gg/G11 pathway (*Ptger3, Tbxa2r*), coagulation factors (*F2rl3, F2rl2*), and the prostaglandin pathway (*Cyp11a1, Ptger3*). These defects likely caused the compensatory upregulation of the coagulation cascade (*Serpina1b*, *Serpind1*) and the kinin-kallikrein system (*Kng2*) mRNAs accompanied by an increase in fibrin degradation mRNAs (plasmin and plasminogen) in the activated platelets of the *Mtif3* knockout mice. The increase in platelet dense granule proteins was common to both the *Elac2* and *Mtif3* knockout mice, but reduction in the platelet release cytosolic proteins—TLN1, WDR1, CAP1, and TUBA4A—was only found in the *Mtif3* knockout mice. Megakaryocyte colony assays revealed significant reduction in the proliferation and differentiation of hematopoietic progenitors into colonies in semi-solid medium in response to cytokine stimulation in the *Ptcd1* and *Mtif3* knockout mice (Figure S8). In contrast, the proliferation of megakaryocytes in the *Elac2* knockout mice was not significantly affected, suggesting that the transcriptional increase in chemotaxis-related genes contributed to the colony-forming ability in the absence of ELAC2. These data provide additional support for megakaryocyte and platelet linked defects in the *Ptcd1* and *Mtif3* knockout mice, compared to the *Elac2* knockout mice that had a platelet-specific defect. Although mitochondrial

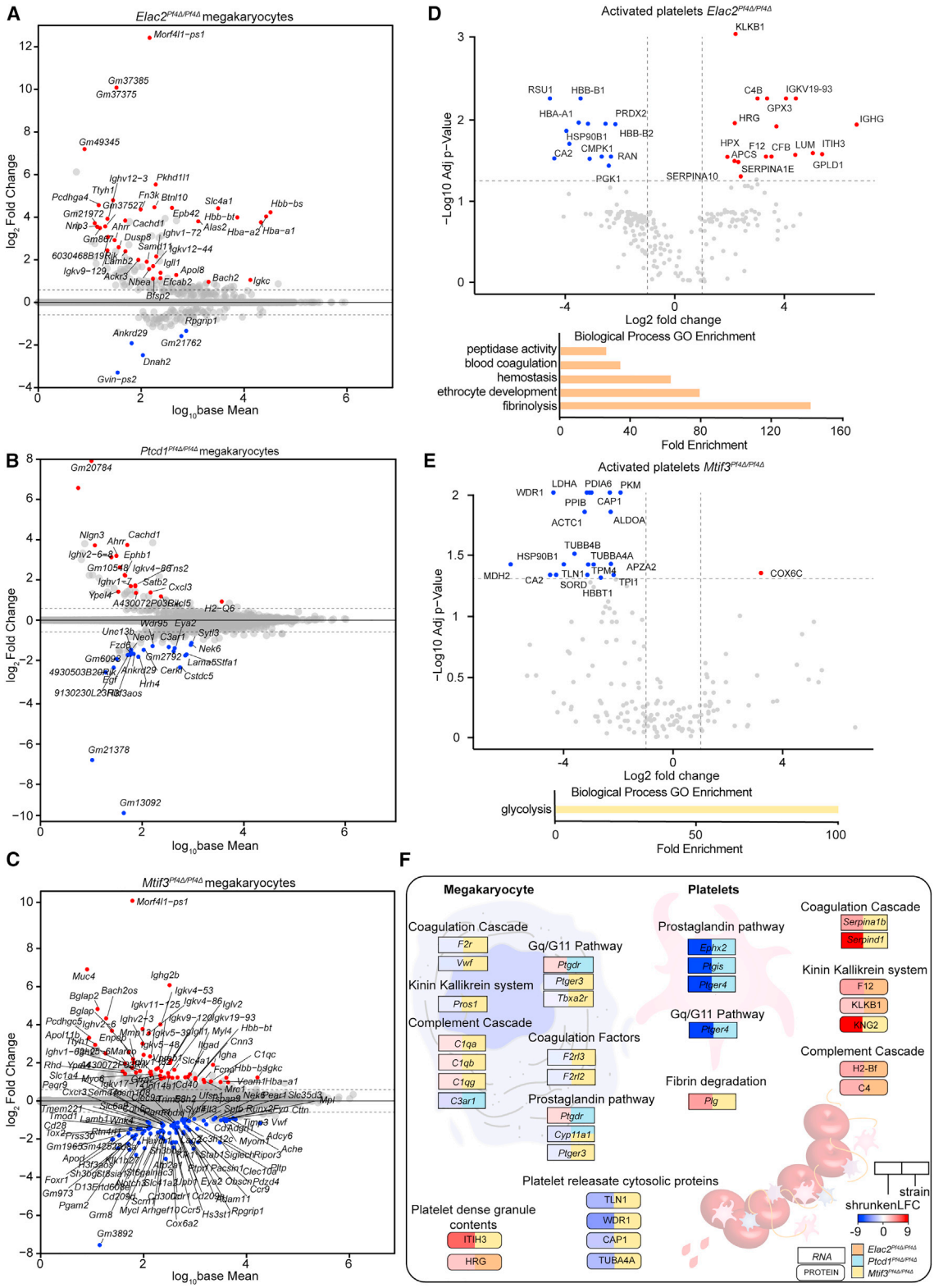

Figure 6. Loss of mitochondrial RNA-binding proteins causes transcriptome and proteome changes that lead to defects in blood coagulation

(A–C) MA plots (log_2 fold change versus the mean normalized count across all samples) showing differential gene expression changes in megakaryocytes isolated from *Elac2* (A), *Ptcd1* (B), and *Mtif3* (C) knockout mice relative to control mice show significantly increased (red) and decreased (blue) genes. Gene expression changes with an FSOS s-value <0.01 and |lfc| >log_2(1.5) were considered significant with n = 3 mice for each experimental group.

(legend continued on next page)

gene expression is required for blood clotting, we show that thrombocytopenia can develop via different pathways depending on the specific requirements for mitochondrial RBPs within megakaryocytes or platelets and their roles in RNA metabolism.

DISCUSSION

Mitochondrial function is crucial for the health and lifespan of platelets, as high energy levels generated by OXPHOS are required for platelet responses to environmental stresses and blood vessel damage.[6] OXPHOS function is dependent on the coordinated regulation of mitochondrial and nuclear gene expression.[7] Defects in mitochondrial bioenergetics causing reduced oxygen consumption, low membrane potential, and an increase in reactive oxidative species have been shown to reduce platelets in leukemia patients[24] and in Pearson's Syndrome, a mitochondrial disorder that primarily affects the pancreas and the hematopoietic stem cells.[25] Although anucleate platelets contain mitochondria and the nuclear transcriptome from mature megakaryocytes, the requirement for mitochondrial gene expression and how this contributes to platelet number and function were not known. Here we show that platelet-specific loss of proteins involved in mitochondrial RNA metabolism (ELAC2 and PTCD1) and protein synthesis (MTIF3) causes thrombocytopenia. Furthermore, we show that mitochondrial gene expression is required for platelet formation from megakaryocytes and for platelet activation, lifespan, and blood coagulation. Our findings indicate that platelets contain nuclear-encoded mitochondrial proteins that can support autonomous mitochondrial gene expression without the requirement for their transcription since platelets are devoid of a nucleus.

Thrombocytopenia may be a consequence of bone marrow defects or as a direct result of damage to circulating platelets.[15] Reticulated platelet numbers can be an indicator of megakaryopoiesis with a low percentage of RPs associated with decreased bone marrow function.[15] Increased levels of RPs revealed that loss of mature platelets and reduced platelet lifespan, but not bone marrow failure, were the most likely causes of thrombocytopenia in the absence of key mitochondrial RBPs. However, platelet count does not always correlate with megakaryocyte number,[26] as seen previously where *Nxf1* mutations in a mouse caused thrombocytopenia as a result of decreased platelet lifespan but not megakaryocyte number.[27] Similarly, in mice lacking ELAC2, a low platelet count was observed despite normal megakaryocyte proliferation and differentiation. In contrast, loss of PTCD1 or MTIF3 impaired megakaryocyte proliferation, suggesting that each of these proteins and mitochondrial translation are important for megakaryocyte function. Although mature megakaryocytes stop proliferating, their DNA content can expand,[28] and loss of each of the three RBPs increased ploidy, likely as a compensatory response to the low platelet numbers.

Reduction of the complement cascade was the unifying change in the three different models of thrombocytopenia; however, each of them had different transcriptional and proteome changes that were likely specific consequences related to the function of each protein. Transcriptional activation of chemotaxis required for wound healing[29] could mitigate defects in mitochondrial RNA processing in the absence of ELAC2 in megakaryocytes, whereas in activated platelets, proteins that regulate blood coagulation, hemostasis, and fibrinolysis were elevated in an attempt to compensate for platelet dysfunction. Loss of PTCD1 caused transcriptional changes in the activated platelets related to protein synthesis, whereas the greatest number of changes were in response to defects in mitochondrial translation initiation, suggesting the protein synthesis in mitochondria is important for platelet function to maintain vascular reliability and hemostatic plug formation. Reduced expression of prostaglandin pathway regulators (Figure 6) can compromise thrombus formation[30] in combination with the reduced numbers of platelets available, further confirming that both platelet numbers and function are necessary for hemostasis. The activation potential of platelets exposed to a panel of agonists revealed reduced sensitivity to AYPGKF in the *Elac2* and *Mtif3* mice, indicating loss of PAR4 signaling. An additional G protein-coupled receptor defect was seen in the *Ptcd1* mice supported by reduced response to ADP, which exposes the fibrinogen binding site on the membrane glycoprotein GPIIb/IIIa complex required for shape change, release of granule contents, and aggregation.[31] In addition, the reduced response to arachidonic acid in the *Mtif3* knockout mice indicated an inability to produce thromboxanes, which are vital in clot formation.[32] We conclude that ELAC2, PTCD1, and MTIF3 are required for platelet aggregation during coagulation.

We show here that impaired mitochondrial gene regulation can contribute to bleeding disorders, and defects in nuclear genes encoding proteins that regulate the mtDNA can result in megakaryocyte or platelet defects. We show that expression of mitochondrial RNAs is required for platelet function during coagulation, opening the way to investigate defects in hemostasis in genetic disorders that are a consequence of mitochondrial dysfunction.

Limitations of the study

Mitochondrial respiration studies would be an advantageous addition to evaluate the respiratory capacity of platelets; however, due to their relative rarity, there are limitations with the availability of material from platelets. In addition, future work

(D and E) Quantitative mass spectrometry was used to identify significantly increased (red) or decreased proteins (blue) in activated platelets isolated from *Elac2* (D) and *Mtif3* (E) knockout mice and treated with 250 μM AYPGKF agonist. ANOVA p values less than 0.01 and log fold change less than −1 and greater than +1 were used to identify significantly changing proteins with n = 3 mice for each experimental group.

(F) PathVisio was used to visualize transcriptome and proteome changes in megakaryocytes and activated platelets. Loss of ELAC2 resulted in altered gene expression in activated platelet dense granule contents, the complement cascade, and the kinin-kallikrein system. Loss of PTCD1 resulted in altered expression of genes involved in the complement cascade, Gq/G11 pathway, and the prostaglandin pathway. Loss of MTIF3 caused changes in the coagulation cascade, the kinin-kallikrein system, complement cascade, Gq/G11 pathway, coagulation factors, and the prostaglandin pathway in megakaryocytes and defects in platelet releasate cytosolic proteins, platelet dense granule contents, and fibrin degradation as well as the coagulation cascade and kinin-kallikrein system.

could focus on identifying the exact signaling cascades that bridge responses from defects in mitochondrial gene expression and transcriptional activation or repression and downstream cytoplasmic signaling cascades.

STAR★METHODS

Detailed methods are provided in the online version of this paper and include the following:

- KEY RESOURCES TABLE
- RESOURCE AVAILABILITY
  - Lead contact
  - Materials availability
  - Data and code availability
- EXPERIMENTAL MODEL AND STUDY PARTICIPANT DETAILS
  - Animal models
- METHOD DETAILS
  - PCR
  - Whole blood measurements and blood films
  - Platelet isolation
  - Isolation of bone marrow
  - Isolation of splenocytes
  - Isolation of single cell suspension from lungs
  - Megakaryocyte enrichment from mouse bone marrow and FACS sorting
  - Cytospins
  - Mitochondrial staining
  - Apoptosis assay
  - Agonist panel assays
  - Flow cytometry analyses
  - Ploidy analysis of megakaryocytes
  - ERK signaling assay
  - Immunoblotting
  - Megakaryocyte colony assays
  - Proplatelet assay
  - Tail bleed assay
  - Reticulated platelet labeling
  - Activation of isolated platelets for proteomics and RNA-seq
  - Peptide digestion and clean-up for label-free mass spectrometry
  - LC-MS/MS analysis
  - RNA isolation
  - RNA-seq
  - Gene ontology
- QUANTIFICATION AND STATISTICAL ANALYSIS

SUPPLEMENTAL INFORMATION

Supplemental information can be found online at https://doi.org/10.1016/j.celrep.2023.113312.

ACKNOWLEDGMENTS

This project was supported by fellowships and project grants from the National Health and Medical Research Council (GNT2017515 to T.R. and GNT1058442, GNT1045677, GNT1041582, GNT1023460, GNT 1005030, and GNT1043978 to A.F. and O.R.), the Australian Research Council (DP180101656 to A.F. and O.R.), the Mito Foundation (to T.R.) and the Cancer Council Western Australia (to O.R. and A.F.). T.R. was a Raine/Bright Spark Foundation Research Fellow, a CSIRO FSP Synthetic Biology Research Fellow, and is currently a NHMRC EL1 Investigator. J.B. is supported by UWA Postgraduate Scholarships. We thank Jennifer Beaumont for technical assistance, and we thank Amandeep Kaur and Elizabeth Gardiner for the polyploidy assay protocol.

AUTHOR CONTRIBUTIONS

O.R. and A.F. conceived the project. O.R., A.F., T.R., and J.E. designed the experiments. All authors conducted and analyzed the experiments. A.F. and T.R. wrote the manuscript, and the other authors edited and approved the manuscript.

DECLARATION OF INTERESTS

The authors declare no competing interests.

Received: June 15, 2022
Revised: July 20, 2023
Accepted: October 5, 2023
Published: October 25, 2023

REFERENCES

1. Rondina, M.T., and Weyrich, A.S. (2015). Regulation of the genetic code in megakaryocytes and platelets. J. Thromb. Haemost. *13*, S26–S32.
2. Lefrançais, E., Ortiz-Muñoz, G., Caudrillier, A., Mallavia, B., Liu, F., Sayah, D.M., Thornton, E.E., Headley, M.B., David, T., Coughlin, S.R., et al. (2017). The lung is a site of platelet biogenesis and a reservoir for hematopoietic progenitors. Nature *544*, 105–109.
3. Ng, A.P., Kauppi, M., Metcalf, D., Hyland, C.D., Josefsson, E.C., Lebois, M., Zhang, J.-G., Baldwin, T.M., Di Rago, L., Hilton, D.J., and Alexander, W.S. (2014). Mpl expression on megakaryocytes and platelets is dispensable for thrombopoiesis but essential to prevent myeloproliferation. Proc. Natl. Acad. Sci. USA *111*, 5884–5889.
4. Tilburg, J., Becker, I.C., and Italiano, J.E. (2022). Don't you forget about me(gakaryocytes). Blood *139*, 3245–3254.
5. Baccarelli, A.A., and Byun, H.M. (2015). Platelet mitochondrial DNA methylation: A potential new marker of cardiovascular disease. Clin. Epigenet. *7*, 44–49.
6. Melchinger, H., Jain, K., Tyagi, T., and Hwa, J. (2019). Role of Platelet Mitochondria: Life in a Nucleus-Free Zone. Front. Cardiovasc. Med. *6*, 153.
7. Rackham, O., and Filipovska, A. (2022). Organization and expression of the mammalian mitochondrial genome. Nat. Rev. Genet. *23*, 606–623.
8. Lopez Sanchez, M.I., Mercer, T.R., Davies, S.M., Shearwood, A.-M.J., Nygård, K.K., Richman, T.R., Mattick, J.S., Rackham, O., and Filipovska, A. (2014). RNA processing in human mitochondria. Cell Cycle *10*, 2904–2916.
9. Holzmann, J., Frank, P., Löffler, E., Bennett, K.L., Gerner, C., and Rossmanith, W. (2008). RNase P without RNA: Identification and Functional Reconstitution of the Human Mitochondrial tRNA Processing Enzyme. Cell *135*, 462–474.
10. Siira, S.J., Rossetti, G., Richman, T.R., Perks, K., Ermer, J.A., Kuznetsova, I., Hughes, L., Shearwood, A.-M.J., Viola, H.M., Hool, L.C., et al. (2018). Concerted regulation of mitochondrial and nuclear non-coding RNAs by a dual-targeted RNase Z. EMBO Rep. *19*, 461988–e46218.
11. Rudler, D.L., Hughes, L.A., Perks, K.L., Richman, T.R., Kuznetsova, I., Ermer, J.A., Abudulai, L.N., Shearwood, A.-M.J., Viola, H.M., Hool, L.C., et al. (2019). Fidelity of translation initiation is required for coordinated respiratory complex assembly. Sci. Adv. *5*, eaay2118.
12. Vafai, S.B., and Mootha, V.K. (2013). A Common Pathway for a Rare Disease? Science *342*, 1453–1454.

13. Perks, K.L., Rossetti, G., Kuznetsova, I., Hughes, L.A., Ermer, J.A., Ferreira, N., Busch, J.D., Rudler, D.L., Spåhr, H., Schöndorf, T., et al. (2018). PTCD1 Is Required for 16S rRNA Maturation Complex Stability and Mitochondrial Ribosome Assembly. Cell Rep. *23*, 127–142.

14. Perks, K.L., Ferreira, N., Richman, T.R., Ermer, J.A., Kuznetsova, I., Shearwood, A.-M.J., Lee, R.G., Viola, H.M., Johnstone, V.P.A., Matthews, V., et al. (2017). Adult-onset obesity is triggered by impaired mitochondrial gene expression. Sci. Adv. *3*, e1700677.

15. Buttarello, M., Mezzapelle, G., Freguglia, F., and Plebani, M. (2020). Reticulated platelets and immature platelet fraction: Clinical applications and method limitations. Int. J. Lab. Hematol. *42*, 363–370.

16. Henriksen, R.A., and Hanks, V.K. (2002). PAR-4 Agonist AYPGKF Stimulates Thromboxane Production by Human Platelets. Arterioscler. Thromb. Vasc. Biol. *22*, 861–866.

17. Yip, C., Linden, M.D., Attard, C., Monagle, P., and Ignjatovic, V. (2015). Platelets from children are hyper-responsive to activation by thrombin receptor activator peptide and adenosine diphosphate compared to platelets from adults. Br. J. Haematol. *168*, 526–532.

18. Jin, J., Quinton, T.M., Zhang, J., Rittenhouse, S.E., and Kunapuli, S.P. (2002). Adenosine diphosphate (ADP)–induced thromboxane A2generation in human platelets requires coordinated signaling through integrin integrin alpha(IIb)beta(3) and ADP receptors. Blood *99*, 193–198.

19. Moog, S., Mangin, P., Lenain, N., Strassel, C., Ravanat, C., Schuhler, S., Freund, M., Santer, M., Kahn, M., Nieswandt, B., et al. (2001). Platelet glycoprotein V binds to collagen and participates in platelet adhesion and aggregation. Blood *98*, 1038–1046.

20. Weyrich, A.S., Dixon, D.A., Pabla, R., Elstad, M.R., McIntyre, T.M., Prescott, S.M., and Zimmerman, G.A. (1998). Signal-dependent translation of a regulatory protein, Bcl-3, in activated human platelets. Proc. Natl. Acad. Sci. USA *95*, 5556–5561.

21. Rhaleb, N.-E., Yang, X.-P., and Carretero, O.A. (2011). The kallikrein-kinin system as a regulator of cardiovascular and renal function. Compr. Physiol. *1*, 971–993.

22. Park, J.-G., Yoo, J.-Y., Jeong, S.-J., Choi, J.-H., Lee, M.-R., Lee, M.-N., Hwa Lee, J., Kim, H.C., Jo, H., Yu, D.-Y., et al. (2011). Peroxiredoxin 2 Deficiency Exacerbates Atherosclerosis in Apolipoprotein E–Deficient Mice. Circ. Res. *109*, 739–749.

23. Vaitkevicius, H., Turner, I., Spalding, A., and Lockette, W. (2002). Chloride increases adrenergic receptor-mediated platelet and vascular responses. Am. J. Hypertens. *15*, 492–498.

24. Baaten, C.C.F.M.J., Moenen, F.C.J.I., Henskens, Y.M.C., Swieringa, F., Wetzels, R.J.H., van Oerle, R., Heijnen, H.F.G., Ten Cate, H., Holloway, G.P., Beckers, E.A.M., et al. (2018). Impaired mitochondrial activity explains platelet dysfunction in thrombocytopenic cancer patients undergoing chemotherapy. Haematologica *103*, 1557–1567.

25. Pearson, H.A., Lobel, J.S., Kocoshis, S.A., Naiman, J.L., Windmiller, J., Lammi, A.T., Hoffman, R., and Marsh, J.C. (1979). A new syndrome of refractory sideroblastic anemia with vacuolization of marrow precursors and exocrine pancreatic dysfunction. J. Pediatr. *95*, 976–984.

26. Bernard, J.J., Seweryniak, K.E., Koniski, A.D., Spinelli, S.L., Blumberg, N., Francis, C.W., Taubman, M.B., Palis, J., and Phipps, R.P. (2009). Foxp3 Regulates Megakaryopoiesis and Platelet Function. Arterioscler. Thromb. Vasc. Biol. *29*, 1874–1882.

27. Chappaz, S., Law, C.W., Dowling, M.R., Carey, K.T., Lane, R.M., Ngo, L.H., Wickramasinghe, V.O., Smyth, G.K., Ritchie, M.E., and Kile, B.T. (2020). Germline heterozygous mutations in Nxf1 perturb RNA metabolism and trigger thrombocytopenia and lymphopenia in mice. Blood Adv. *4*, 1270–1283.

28. Zhang, X., Fu, H., Xu, L., Liu, D., Wang, J., Liu, K., Huang, X., Li, A., Wang, Z.k., and Zhao, Y. (2011). Prolonged thrombocytopenia following allogeneic hematopoietic stem cell transplantation and its association with a reduction in ploidy and an immaturation of megakaryocytes. Biol. Blood Marrow Transplant. *17*, 274–280.

29. Kundra, V., Escobedo, J.A., Kazlauskas, A., Kim, H.K., Rhee, S.G., Williams, L.T., and Zetter, B.R. (1994). Regulation of chemotaxis by the platelet-derived growth factor receptor-beta. Nature *367*, 474–476.

30. Ma, H., Hara, A., Xiao, C.Y., Okada, Y., Takahata, O., Nakaya, K., Sugimoto, Y., Ichikawa, A., Narumiya, S., and Ushikubi, F. (2001). Increased bleeding tendency and decreased susceptibility to thromboembolism in mice lacking the prostaglandin E receptor subtype EP(3). Circulation *104*, 1176–1180.

31. Lowe, G.C., Fickowska, R., Al Ghaithi, R., Maclachlan, A., Harrison, P., Lester, W., Watson, S.P., Myers, B., Clark, J., and Morgan, N.V. (2019). Investigation of the contribution of an underlying platelet defect in women with unexplained heavy menstrual bleeding. Platelets *30*, 56–65.

32. Zhou, L., and Schmaier, A.H. (2005). Platelet Aggregation Testing in Platelet-Rich Plasma. Am. J. Clin. Pathol. *123*, 172–183.

33. Martin, M. (2011). Cutadapt removes adapter sequences from high-throughput sequencing reads. EMBnet. j. *17*, 10–12.

34. Soneson, C., Love, M.I., and Robinson, M.D. (2015). Differential analyses for RNA-seq: transcript-level estimates improve gene-level inferences. F1000Res. *4*, 1521.

35. Love, M.I., Huber, W., and Anders, S. (2014). Moderated estimation of fold change and dispersion for RNA-seq data with DESeq2. Genome Biol. *15*, 550–621.

36. Zhu, A., Ibrahim, J.G., and Love, M.I. (2019). Heavy-tailed prior distributions for sequence count data: removing the noise and preserving large differences. Bioinformatics *35*, 2084–2092.

37. Tiedt, R., Schomber, T., Hao-Shen, H., and Skoda, R.C. (2007). Pf4-Cre transgenic mice allow the generation of lineage-restricted gene knockouts for studying megakaryocyte and platelet function in vivo. Blood *109*, 1503–1506.

38. Salzmann, M., Hoesel, B., Haase, M., Mussbacher, M., Schrottmaier, W.C., Kral-Pointner, J.B., Finsterbusch, M., Mazharian, A., Assinger, A., and Schmid, J.A. (2018). A novel method for automated assessment of megakaryocyte differentiation and proplatelet formation. Platelets *29*, 357–364.

39. Huang, D.W., Sherman, B.T., and Lempicki, R.A. (2009). Bioinformatics enrichment tools: paths toward the comprehensive functional analysis of large gene lists. Nucleic Acids Res. *37*, 1–13.

40. Huang, D.W., Sherman, B.T., and Lempicki, R.A. (2009). Systematic and integrative analysis of large gene lists using DAVID bioinformatics resources. Nat. Protoc. *4*, 44–57.

STAR★METHODS

KEY RESOURCES TABLE

REAGENT or RESOURCE	SOURCE	IDENTIFIER
Antibodies		
Anti-mouse CD61-conjugated MicroBeads	Miltenyi-Biotec	130-109-678
CD41-FITC	Becton Dickinson	553848
MT-COX2	Proteintech	55070-1-AP
NDUFB8	Thermofisher	459210
ATP5A1	Thermofisher	43–9800
GAPDH	Cell Signaling	2118
PE Hamster Anti-Mouse CD61	Becton Dickinson	553347
CD62P Selection Monoclonal Antibody APC	Thermofisher	17-0626-82
Alexa Fluor 488 anti-mouse CD41	Biolegend	133908
Alpha tubulin monoclonal antibody eFluor 615	Thermofisher	42-4502-82
Anti-mouse CD61 conjugated microbeads	Miltenyi-Biotec	130-109-678
Alexa Fluor 647 Annexin V	Australian Biosearch	640912
IR Dye 800CW Goat Anti-Rabbit IgG	LI-COR	926–32211
IR Dye 680LT Goat Anti-Mouse IgG	LI-COR	926–68020
Chemicals, peptides, and recombinant proteins		
TRIzol Reagent	Invitrogen	15596018
Prostaglandin I2 sodium salt	Sigma	P6188
Collagenase	Sigma	C2139
Propidium Iodide	Sigma	P4170
Acethlthiocholine Iodide	Sigma	A5751
Mitotracker Green FM	Thermofisher	M7514
ABT-737	Sigma	AMBH46A966B9
TPO	StemCell	78210
IL6	StemCell	78050.1
IL11	StemCell	78025.1
IL3	StemCell	78042.1
Critical commercial assays		
Quick Dip Staining Kit	Thermofisher	FNNQUICKDIPKIT500
Megacult-C Complete Kit without cytokines	StemCell	04970
Direct-zol RNA Microprep kit	Zymo Research	R2062
ERK1/ERK2 (Total/Phospho) Multispecies InstantOne ELISA Kit	ThermoFisher	85-86013-11
Deposited data		
Gene Expression Omnibus (GEO)	This paper	GSE206543
PRIDE	This paper	PXD045688
Experimental models: Organisms/strains		
Pf4-Cre mice	Professor Benjamin Kile	PMID: 24632563
ELAC2 KO mice	This paper	N/A
PTCD1 KO mice	This paper	N/A
MTIF3 KO mice	This paper	N/A
Oligonucleotides		
PCR primers Elac2 forward 5′-tcgtcggcagcgtcagatgtgtataagagacag AAAAGGCGCATAACGATACCAC-3′	IDT	N/A

(*Continued on next page*)

Continued

REAGENT or RESOURCE	SOURCE	IDENTIFIER
PCR primers Elac2 reverse 5′-gtctcgtgggctcggagatgtgtataagagacag GCACTAGCTGCTCTGAATGAAC-3′	IDT	N/A
PCR primers Ptcd1 forward 5′-tcgtcggcagcgtcagatgtgtataagagacag GAGTAGACGGCGCAAGGATG-3′	IDT	N/A
PCR primers Ptcd1 reverse 5′-gtctcgtgggctcggagatgtgtataagagacag TCGATGAGAACTGCAGGAGG-3′	IDT	N/A
PCR primers Mtif3 forward 5′-tcgtcggcagcgtcagatgtgtataagagacag ACCCCATGCGTGTATTAAAGG-3′	IDT	N/A
PCR primers Mtif3 reverse 5′-gtctcgtgggctcggagatgtgtataagagacag ATCTGGTGTGAACTGATGGC-3′	IDT	N/A
Software and algorithms		
FACSDiva v6.1.3	Becton Dickinson	643629
Nikon NIS-Elements confocal v8 imaging software		N/A
CellProfiler 3.0.0		http://cellprofiler.org/
Trim Galore (–fastqc –paired –nextera –clip_R1 1 –clip_R2 1) using Cutadapt 1.18 and FastQC 0.11.9	Martin et al.[33]	https://github.com/FelixKrueger/TrimGalore; https://github.com/s-andrews/FastQC
tximport	Soneson et al.[34]	26925227
DESeq2	Love et al.[35]	25516281
apeglm	Zhu et al.[36]	30395178
DAVID		https://david.ncifcrf.gov/
GraphPad Prism 10	GraphPad	https://www.graphpad.com/

RESOURCE AVAILABILITY

Lead contact

Further information and reasonable requests for resources and reagents should be directed to and will be fulfilled by the lead contact, Aleksandra Filipovska (aleksandra.filipovska@uwa.edu.au).

Materials availability

Reagents generated in this paper can be made available subject to an MTA completion.

Data and code availability

- Genomic data have been deposited to the Gene Expression Omnibus (GEO) under accession GSE206543 and proteomic data have been deposited to PRIDE under accession number PXD045688 and all data are freely accessible.
- This paper does not report original code.
- Any additional information required to reanalyze the data reported in this paper is available for the lead contact upon request.

EXPERIMENTAL MODEL AND STUDY PARTICIPANT DETAILS

Animal models

The generation of *Elac2* $^{loxP/loP}$,[10] *Ptcd1*$^{loxP/loxP}$,[14] *Mtif3* $^{loxP/loxP}$[11] and *Pf4-Cre*[37] transgenic mice have been previously described. *Elac2* $^{loxP/loxP}$, *Ptcd1* $^{loxP/loxP}$ and *Mtif3* $^{loxP/loxP}$ mice on a C57BL/6N background were crossed with *Pf4*-Cre mice to generate control (L/L) and megakaryocyte specific deletions (L/L, cre+) of each of the three genes. Mice were housed in standard cages (45 cm × 29 cm x 12 cm) under a 12-h light/dark schedule (lights on 7:00 a.m. to 7:00 p.m.) in controlled environmental conditions of 22° ± 2°C and 50 + 10% relative humidity and fed a normal chow diet (Rat & Mouse Chow, Specialty Foods, Glen Forrest, Western Australia), and water was provided *ad libitum*. These studies used both male and female mice and the presented data are from male mice that were 4 weeks of age. The study was approved by the Animal Ethics Committee of the University of Western Australia

(UWA) and performed in accordance with Principles of Laboratory Care [National Health and Medical Research Council (NHMRC), *Australian Code for the Care and Use of Animals for Scientific Purposes*, ed. 8, 2013].

METHOD DETAILS

PCR

DNA extraction was performed using TRIzol Reagent (Invitrogen 15596026, 15596018) as per manufacturer's instructions, on enriched megakaryocytes isolated from mouse bone marrow. DNA was then concentrated and cleaned using a DNA Clean and Concentrator kit (Zymo Research D4004) as per manufacturer's instructions. Primers were synthesized by IDT, for *Elac2*: 5′-tcgtcggcagcgtcagatgtgtataagagacagAAAAGGCGCATAACGATACCAC-3′ and 5′-gtctcgtgggctcggagatgtgtataagagacagGCAC TAGCTGCTCTGAATGAAC-3′, for *Ptcd1*: 5′-tcgtcggcagcgtcagatgtgtataagagacagGAGTAGACGGCGCAAGGATG-3′ and 5′-gtctcg tgggctcggagatgtgtataagagacagTCGATGAGAACTGCAGGAGG-3′, for *Mtif3*: 5′-tcgtcggcagcgtcagatgtgtataagagacagACCCCATGC GTGTATTAAAGG-3′ and 5′-gtctcgtgggctcggagatgtgtataagagacagATCTGGTGTGAACTGATGGC-3′.

Whole blood measurements and blood films

Approximately 60 μL of whole blood was collected via lateral artery tail bleeds into K2EDTA BD microtainer blood collection tubes for analysis with the Hemavet 950. A capillary tube was used to draw up blood from the EDTA tube to create blood films which were stained with the Quick Dip Staining kit (ThermoFisher).

Platelet isolation

Mice were anesthetised with methoxyflurane and blood obtained by cardiac puncture into a syringe containing 100 μL of Astr Jandl citrate-based anticoagulant (85 mM sodium citrate dihydrate, 69 mM citric acid, 20 mg/mL glucose, pH 4.6). Blood was centrifuged at 125 *g* for 8 min at room temperature (brake and acceleration off). The platelet rich plasma was transferred to a new tube with 8 μL of 50 μM prostaglandin (if platelets were not subsequently treated with agonists) and 300 μL platelet wash buffer (140 mM NaCl, 5 mM KCl, 12 mM sodium citrate, 10 mM glucose, 12.5 mM sucrose, pH 6.0) and centrifuged at 125 *g* for 8 min at room temperature. The supernatant was transferred to another tube and 300 μL platelet wash buffer added and centrifuged at 860 *g* for 5 min at room temperature. The platelet pellet was snap frozen for proteomic analyses or resuspended in 80 μL of platelet buffer (10 mM HEPES, 140 mM NaCl, 3 mM KCl, 0.5 mM $MgCl_2$ hexahydrate, 0.5 mM $NaHCO_3$, 10 mM glucose, pH 7.4) for FACS analyses.

Isolation of bone marrow

Mouse femurs were removed and cleaned of connective tissue. The ends of the femurs were clipped to expose the bone marrow and a 21-gauge needle used to flush the marrow into a 10 mL tube using IMDM (Iscove's Modified Dulbecco's Medium). A single cell suspension was created by passing the marrow through the 21-gauge needle and cells were pelleted by centrifugation at 450*g* for 5 min. The pellet was washed with cold IMDM and vortexed before pelleting again at 450 *g* for 5 min.

Isolation of splenocytes

To generate a single cell suspension, spleens were removed and pressed through a 70 μm cell strainer using the end of a 1 mL syringe plunger. The cell strainer mesh was washed with IMDM into a 50 mL centrifuge tube and cells were pelleted at 450 *g* for 5 min at room temperature.

Isolation of single cell suspension from lungs

The right lung of each mouse was minced and dissociated using a gentleMACS C-tube (Miltenyi) in the presence of 2.5 mg Collagenase (Sigma C2139) and 20 μL DNase I (10,000 U/ml) in 5 mL HEPES buffer (10 mM HEPES-NaOH pH 7.4, 150 mM NaCl, 5 mM KCl, 1 mM $MgCl_2$, 1.8 mM $CaCl_2$). Tissue was dissociated using a gentleMACS Octo Dissociator (Miltenyi on the 37C_m_LDK_1 program. A single cell suspension was created by passing through a 100 μm mesh cell strainer and cells were pelleted at 300 *g* for 10 min.

Megakaryocyte enrichment from mouse bone marrow and FACS sorting

Freshly derived bone marrow cells were collected from the tibia and femur of mice in ice-cold Buffer A (PBS: Mg^{2+}- and Ca^{2+}-free with 2% FBS and 5 mM EDTA) and centrifuged at 300 *g*, 5 min at RT. Pellets were incubated in 2 mL Red blood cell lysis buffer (17 mM Tris-HCl, pH7.6, containing 144 mM NH_4Cl) for 3 min at 4°C. Buffer A was added to a total of 40 mL and samples were filtered through a 100 μm nylon cell strainer and centrifuged at 300x *g* for 5 min. The cell pellet was resuspended in 1 mL of Buffer A and cell counts were performed using a propidium iodide solution (1 μg/ml final concentration in Buffer A). Cells were collected by centrifugation and resuspended in PBS +2% FBS at 10^7 cells/80 μL. Anti-mouse CD61-conjugated MicroBeads (Miltenyi-Biotec, cat. no. 130-109-678) were added to cells and incubated in the dark for 15 min at 4°C. Following incubation PBS +2% FBS was added to a total of 500 μL. For megakaryocyte (Mk) cell enrichment the Miltenyi MACS Separator was used according to the manufacturer's instructions. LS columns (Miltenyi, cat. no. 130-042-401) were used for bead separation and were primed by rinsing 3 times with 3 mL PBS +2% FBS and the cell suspensions were applied to columns and the flow through collected. Columns were washed with 3 × 3 mL PBS +2% FBS and placed into a collection tube. Captured magnetic CD61 positive beads were flushed out by firmly pushing the

plunger 3 times with 5 mL PBS +2% FBS and pelleting at 300 *g* for 5 min at RT. Cell pellet was resuspended in 250 μL Buffer A. Tubes were prepared as follows: 10 μL of the cell suspension was used for each single stain control (PI, unstained, CD41-FITC) to a total of 100 μL Buffer A and the remaining cells were stained with 2.5 μL CD41-FITC (BD, cat. no. 553848) and incubated for 30 min at 4°C in the dark. Following incubation, 300 μL of Buffer A was added and tubes were centrifuged at 300 *g*, 5 min at RT. Pellets were washed and resuspended in 300 μL live-dead stain with propidium iodide for: PI single color and CD41-FITC stains, or Buffer A for: unstained and CD41-FITC single color tubes. FACs analysis was performed on a FACS ARIA II (BD Biosciences). Mk cells were gated on live, high FSC and CD41 positive staining. Mk cells were sorted based on the profile of a pure Mk cell population and pellets collected.

Cytospins

Single cell suspensions of bone marrow, spleen and lung cells were centrifuged onto glass slides at 4.5 *g* for 3 min using a Cytospin 2 centrifuge (Shandon Scientific Ltd.) and dried for 20 min at room temperature. Slides were fixed by heating for 5 min at 50°C and stained with acetylthiocholine iodide solution (2 mM acetyltiocholine iodide, 5 mM sodium citrate, 75 mM sodium phosphate, 3 mM copper sulfate, 0.5 mM potassium ferricyanide solution) for 5 h in a humidified chamber. Slides were then fixed in 95% ethanol for 10 min, rinsed in water and air dried before counterstaining with Harris' hematoxylin solution for 30 s. Once stained, slides were dehydrated with xylene in preparation for mounting. Slides were washed for 2 min in 95% ethanol, then washed for 2 min in 100% ethanol. Slides were rinsed with 100% xylene for 2 min and then incubated in fresh 100% xylene for 2 min. Once dry, a coverslip was mounted using DPXMountant for Histology (Sigma-Aldrich). Slides were imaged using a light microscope (Olympus BX51 and Olympus DP80 microscope digital camera).

Mitochondrial staining

Isolated platelets were incubated with 200 nM Mitotracker Green FM for 15 min at 37°C in the dark. After incubation platelets were fixed by adding 600 μL of HEPES saline 1% formaldehyde for 10 min, protected from light. Samples were analyzed on a BD Accuri C6 flow cytometer (BD Biosciences).

Apoptosis assay

Isolated platelets treated with 5 mM ABT-737 or untreated were incubated with 250 ng of Alexa Fluor 647 Annexin V in Annexin V Binding buffer for 15 min at 37°C in the dark. After incubation fixation was performed by adding 600 μL of HEPES saline 1% formaldehyde for at least 10 min, protected from light. Samples were analyzed on a BD Accuri C6 flow cytometer (BD Biosciences).

Agonist panel assays

5 μL of platelets resuspended in 80 μL of platelet buffer (10 mM HEPES, 140 mM NaCl, 3 mM KCl, 0.5 mM $MgCl_2$ hexahydrate, 0.5 mM $NaHCO_3$, 10 mM glucose, pH 7.4) with platelet concentration less than 200 K/μL were aliquoted into tubes containing agonists at low and high concentrations as follows: 50 μM or 250 μM AYPGKF, 2.5 μM or 100 μM ADP, 50 μM or 1 mM arachidonic acid, 20 μg/mL or 80 μg/mL collagen. Each tube was incubated for 15 min at 37°C protected from light with 0.2 μg anti-CD61 PE and anti-CD62P APC in 10 μL Stain buffer with BSA (BD Biosciences Cat 554657). One tube was incubated with 0.2 μg anti-CD61 PE and 0.2 μg mouse IgG1 kappa APC with no agonist as a control. After incubation fixation was performed by adding 600 μL of HEPES saline 1% formaldehyde for at least 10 min, protected from light.

Flow cytometry analyses

Platelet flow cytometry was performed by adapting established methods (Mosawy et al., 2013). Briefly, platelets were identified by characteristic CD61 expression and laser scatter properties using a BD Accuri C6 (BD Biosciences) flow cytometer. A minimum of 10,000 platelets were collected and their CD62P fluorescence measured relative to isotype control, to exclude autofluorescence and non-specific probe binding. The percentage of CD62P-positive platelets relative to the total number of platelets was recorded for each sample condition as a marker of agonist induced granule exocytosis. The results are presented as a fold change from unstimulated control to demonstrate specific agonist response.

Ploidy analysis of megakaryocytes

Freshly derived bone marrow cells were collected in Buffer A (PBS: Mg, Ca free with 2% FBS and 5 mM EDTA) and centrifuged at 17 *g*. Cells were washed and filtered through a MACS 100 μm cell strainer. Cells were stained for 30 min on ice with CD41-FITC megakaryocyte marker (BD Biosciences, cat. no. 553848) or control mouse IgG-FITC, for single color controls and ploidy assessment. Cells were washed in 400 μL CATCH buffer (1 x Hanks Balance Salt Solution, Ca/Mg/phenol red-free (Invitrogen), 3% FBS, 3% BSA, 0.38% sodium citrate, 1 mM adenosine, 2 mM theophylline) and centrifuged at 23 *g* for 5 min at 4°C. Pellets were resuspended in 500 μL CATCH buffer and stained for 30 min at 4°C in the dark with 3 mL of propidium iodide (PI) (Sigma; 50 μg/mL in 0.1% sodium citrate) or 3 mL 0.1% sodium citrate (vehicle) as control. 4 mL of CATCH buffer was added, and the cells centrifuged at 58 *g* for 5 min at 4°C, the supernatant was removed leaving 200–400 μL of buffer for resuspension and incubated for 30 min at RT in the dark with RNase A (Sigma) to a final concentration of 50 μg/mL for FACS analysis on a FACSARIA II (BD Biosciences). FACSDiva v6.1.3 (BD

Biosciences) software was used for analysis and cells were gated on IgG-FITC control and confirmed using a CD41-FITC positive sample. High $CD41^+$ events were counted and the 2N population was based on lymphocyte gate (FSC/SSC plot). Log scale was used for PI events.

ERK signaling assay

Isolated platelets activated with AYPGKF were quantified for levels of phosphorylated and total ERK1/ERK2 using ELISA kit ERK1/ERK2 (Total/Phospho) Multispecies InstantOne ELISA Kit (85-86013-11 ThermoFisher) as per the manufacter's instructions.

Immunoblotting

Specific proteins were detected using rabbit monoclonal antibodies against: MT-COX2 (55070-1-AP), NDUFB8 (459210), ATP5A1 (43–9800) and GAPDH (2118). All primary antibodies were diluted 1:1000 using the Odyssey blocking buffer (LI-COR). IR Dye 800CW Goat Anti-Rabbit IgG or IR Dye 680LT Goat Anti-Mouse IgG (LI-COR) secondary antibodies (diluted 1:10,000) were used and the immunoblots were visualized and quantified using the Odyssey Infrared Imaging System (LI-COR).

Megakaryocyte colony assays

Colony forming unit megakaryocyte (CFU-Mk) assays were performed on bone marrow using the MegaCult-C system (StemCell Technologies) as per the manufacturer's instructions. To 1.7 mL of MegaCult-C medium were added, $2.5x10^5$ bone marrow cells, TPO (50 ng/mL), IL6 (20 ng/mL), IL11 (50 ng/mL), IL3 (10 ng/mL) cytokines. Cells were added to 1.5 mL of cold collagen solution and 0.75 mL of the final culture mixture was distributed into each of two wells of a two double chamber slides (4 chambers in total). Cells were cultured at 37°C in 5% CO_2 for 7 days. CFU-Mks were detected by acetylthiocholine iodide staining as described above (excluding coverslip mounting) and counted using a light microscope.

Proplatelet assay

Femurs and tibias were isolated from mice and the marrow flushed with an isotonic buffer (143 mM NaCl, 5.6 mM KCl, 10 mM HEPES (pH 7.2), 10 mM glucose, 0.4% BSA and 0.2 U/ml apyrase) using a 24-gauge needle to disperse the tissue. Cells were supplemented with 2.67 μM PGI_2 and pelleted at 200 *g* for 10 min, then resuspended in isotonic buffer (without apyrase) with 2 mM $MgCl_2$, 0.2 mM $CaCl_2$ to a final concentration of 10-20 $x10^6$ cells/ml. Cells were plated onto glass coverslips (previously coated in 100 μg/mL fibrinogen and blocked for 1 h in 1% BSA) and allowed to adhere for 5 h at 37°C in a humidified atmosphere. Slides were washed 3 x in PBS for 5 min and fixed in 10% formalin for 10 min at room temperature. Slides were washed again 3x in ice-cold PBS and cells were permeabilized using 0.5% Triton X-100 in PBS for 5 min. Slides were washed again and then blocked for 30 min with 1% BSA in 0.1% Tween 20.

Slides were incubated overnight with anti-mouse CD41-Alexa Fluor 488 (Biolegend) and alpha tubulin eFluor615 (eBioscience) at 4°C in a humidity chamber protected from light. Slides were washed 3x in PBS for 5 min and then stained with phalloidin-Alexa Fluor 555 (Molecular Probes) at 4°C in a humidity chamber protected from light for 20 min, washed again and then counterstained with Hoechst 33342 (Molecular Probes) for 5 min. A PBS rinse was performed, and coverslips were mounted onto slides with Fluoromount-G. Images were taken with a Nikon Ni-E confocal laser-scanning microscope using Nikon NIS-Elements confocal v8 imaging software. Quantification was performed as described previously using the open-source software CellProfiler 3.0.0.[38] Megakaryocytes were categorized as the following subtypes: proplatelet-forming MKs (Form Factor $\leq$0.19), spreading MKs (Form Factor >0.19, Area >6000 μm2), pseudopodia-forming MKs (Form Factor >0.19, Area $\leq$6000 μm2, Compactness >1.25), undifferentiated MKs (Form Factor >0.19, Area $\leq$6000 μm2, Compactness $\leq$1.25).

Tail bleed assay

Tail bleed assays were performed as per (Liu, 2012). Briefly, mice were weighed before and after the procedure to assess blood loss. Anesthesia of animals was maintained by mask inhalation of isoflurane 1–2% isoflurane in 100% oxygen at a flow rate of 2 L/min. A distal 10-mm segment of the tail was amputated, and the tail was immersed in isotonic saline at 37°C. The bleeding time of the animals was monitored for 20 min. Volume of blood loss was calculated using the equation of Lee and Blaufox; blood volume (mL) = 0.06 x loss of body weight (g) +0.77. Bleeding index was calculated as a multiplication of blood loss (mL) and total bleeding time (min).

Reticulated platelet labeling

Whole blood was collected via lateral artery tail bleed into K2EDTA BD microtainer blood collection tubes. Blood was incubated for 15 min at room temperature as follows: (a) 1 μL of blood was incubated with 9 μL IgG diluted 1:40 in PBS, 9 μL CD61 diluted 1:40 in PBS (b) 1 μL of blood was incubated with 9 μL CD61 diluted 1:40 in PBS and (C) 1 μL of blood was incubated with 9 μL CD61 diluted 1:40 in PBS and 50 μL thiazole orange (Sigma) at 0.1 μg/mL. Samples were fixed in 1 mL 1% paraformaldehyde and analyzed immediately by FACS. The percentage of reticulated platelets was calculated by percentage of platelets positively stained for thiazole orange.

Activation of isolated platelets for proteomics and RNA-seq

The platelet pellet was resuspended in 100 μL of 250 μM AYPGKF and incubated at 37°C for 15 min in the dark, then centrifuged at 860 *g* for 5 min at room temperature to separate pellet and activated supernatant. Both pellet and supernatant were snap frozen separately at −80°C for proteomics analyses.

Peptide digestion and clean-up for label-free mass spectrometry

15-20x10^6 platelets were isolated as above. Platelet pellets and supernatants were prepared as described previously.[11] Briefly, platelets were resuspended in lysis buffer [6 M guanidinium chloride, 2.5 mM tris(2-carboxyethyl)phosphine hydrochloride, 10 mM chloroacetamide, and 100 mM tris-HCl]. Following lysis, samples were diluted 1:10 in 20 mM tris-HCl (pH 8.0), and 100 μg of protein was mixed with 1 μg of Trypsin Gold (Promega) and digested overnight at 37°C. Peptides were cleaned with homemade STAGEtips (Empore Octadecyl C18; 3M, Germany) and eluted in 60% acetonitrile/0.1% formic acid buffer. Samples were dried in a SpeedVac (Eppendorf Concentrator plus 5305) at 45°C, the peptides were suspended with 0.1% formic acid, and 1.5 μg of peptides was analyzed by liquid chromatography–tandem mass spectrometry (LC-MS/MS).

LC-MS/MS analysis

Mass spectrometric analysis was performed as described previously.[11] Peptides were separated on a 50-cm-long, 75–μm–internal diameter EASY-spray PepMap C18 column(Thermo Fisher Scientific) using a Dionex UltiMate 3000 Nano-UHPLC system (Thermo Fisher Scientific). The column was maintained at 50°C. Buffers A and B were 0.1% formic acid in water and 0.1% formic acid in acetonitrile, respectively. Peptides were separated on a segmented gradient from 3 to 10% buffer B for 8 min, from 10 to 25% buffer B for 44 min, from 25 to 40% buffer B for 10 min, and from 40 to 95% buffer B for 12 min, at 300 nL/min. Eluting peptides were analyzed on an Orbitrap Fusion mass spectrometer (Thermo FisherScientific). The instrument was operated in a data-dependent ''TopSpeed'' mode, with cycle times of 2 s. The ''Universal Method'' template was used. Peptide precursor mass/charge ratio(m/z) measurements (MS1) were carried out at 60,000 resolution inthe m/z range of 300–1500. The MS1 AGC target was set to 1 × 106, and the maximum injection time was set to 300 ms. Precursor priority was set to ''Most intense,'' and precursors with charge states 2 to 7 onlywere selected for higher-energy collisional dissociation fragmentation. Fragmentation was carried out using 27% collision energy. The m/z values of the peptide fragments were measured in the Orbitrap usingan AGC target of 5 × 10 4 and 40-ms maximum injection time. The option ''Inject ions for All Available Parallelizable Time'' was enabled. Proteome Discoverer (PD; v.2.2.0388; Thermo Fisher Scientific) proteomics software was used to process raw (Xcalibur) MS/MS data.

RNA isolation

RNA was isolated form megakaryocyte or platelet pellets using the Direct-zol RNA Microprep kit (Zymo Research) as per the manufacturer's instructions.

RNA-seq

Libraries were constructed from total RNA isolated from megakaryocytes, resting and activated platelets each from three control and three of each knockout mouse lines using an Illumina Stranded mRNA preparation kit and sequenced using a NovaSeq platform by the Australian Genome Research Facility (AGRF). Sequenced reads were trimmed with Trim Galore (–fastqc –paired –nextera –clip_R1 1 –clip_R2 1) (https://github.com/FelixKrueger/TrimGalore) using Cutadapt 1.18[33] and FastQC 0.11.9 (https://github.com/s-anders/FastQC). Trimmed reads were quantified with Salmon 1.5.2 using the selective alignment procedure (-l A –seqBias –qcBias –validateMappings) against the GENCODE vM27 transcriptome, with custom mitochondrial transcripts (properly merged bicistronic transcript sequences and corrected terminal sequences, and removal of mt-tRNAs). Transcript quantifications were summarised to gene-level with tximport[34] and analyzed for differential gene expression changes with DESeq2,[35] using the apeglm[36] shrinkage estimator and an lfcThreshold of $\log_2(1.5)$. Gene expression changes with an FSOS s-value <0.01 and an absolute $\log_2$ fold change greater than $\log_2(1.5)$ were considered significant. Normalized, strand-specific coverage profiles were generated with deepTools 3.5.0 bamCoverage (–filterRNAstrand [forward/reverse] –samFlagInclude 2 –samFlagExclude 256 –normalizeUsing CPM –exactScaling -bs 1 -of bigwig).

Gene ontology

Gene ontology analysis was performed on differentially expressed genes for significant proteomics or transcriptomics results. DAVID was used to perform statistical overrepresentation tests for biological process ontologies.[39,40]

QUANTIFICATION AND STATISTICAL ANALYSIS

Two-way Student's t-test was used for most analyses (RNAseq and proteomic analyses used statistical analyses as described in the methods above) assuming normal distribution unless otherwise stated, there was no blinding of data, biological replicates were used for all experiments and the sample size is included in the figure legends. All values are means ± SEM and n represents number of mice used as indicated in each figure legend. GraphPad Prism was used for all statistical analyses.